HHS Public Access

Author manuscript

J Biomed Nanotechnol. Author manuscript; available in PMC 2017 August 24.

Published in final edited form as:

J Biomed Nanotechnol. 2017 April ; 13(4): 355–366. doi:10.1166/jbn.2017.2353.

Encapsulation of Anticancer Drugs (5-Fluorouracil and Paclitaxel) into Polycaprolactone (PCL) Nanofibers and *In Vitro* Testing for Sustained and Targeted Therapy

Sakib Iqbal[1], **Mohammad H. Rashid**[2], **Ali S. Arbab**[2], and **Mujibur Khan**[1,*]

[1]Mechanical Engineering, Georgia Southern University, Statesboro, GA

[2]Georgia Cancer Center; Augusta University, Augusta, GA

Abstract

We report a continuous nanoscale encapsulation of cancer drugs 5-Fluorouracil (FU) and Paclitaxel into biocompatible polycaprolactone (PCL) nanofibers (NFs) using core-sheath electrospinning process. A high potential electric field of 19–23.2 kV was used to draw a compound solution jet from a specialized coaxial spinneret. Using of DMF in both core and Sheath resulted in NFs within 50–160 nm along with large beaded structures. Addition of Trichloromethane (TCM) or Trifluoroethanol (TFE) in sheath turned NFs in more uniform and thin fiber structure. The diameter range for paclitaxel encapsulated fibers was 22–90 nm with encapsulation efficiency of 77.5% and the amount of drug was only 4 to 5% of sheath polymer. Addition of PVA within core resulted drug nanocrystal formation outside of sheath and poor encapsulation efficiency (52%) with rapid initial release (52–53%) in first 3 days. Drug release test of NFs in different pH exhibited increase of release rate with the decrease of media pH. *In-vitro* cell viability test with FU encapsulated NFs in human prostatic cancer PC3 cells exhibited 38% alive cells at 5 μM concentration while in pristine FU 43% cells were alive. Paclitaxel encapsulated NFs with breast cancer cells also exhibited increased efficacy in comparison to pristine anticancer drugs. Continuous decrease of cell density indicated the slow release of cancer drugs from the NFs. Both PCL+Paclitaxel and PCL+5FU treated conditions caused breast cancer cell death between 40% to 50%.

Keywords

Nanofibers; Paclitaxel; 5-Fluorouracul; Encapsulation; Electrospinning; Cytotoxicity

INTRODUCTION

Cancer occurs at a molecular level when multiple subsets of genes undergo genetic alterations,[1–3] either activation of oncogenes or inactivation of tumor suppressor genes. Then malignant proliferation of cancer cells, tissue infiltration, and dysfunction of organs will appear.[4, 5] Tumor tissues are characterized with active angiogenesis and high vascular density, which keep blood supply for their growth, but with a defective vascular architecture.

*Author to whom correspondence should be addressed. mkhan@georgiasouthern.edu.

The inherent complexity of tumor microenvironment and the existence of P-glycoprotein (P-gp) usually act as barriers to traditional chemotherapy by preventing drug from reaching above threshold value inside tumor cells. Combined with poor lymphatic drainage, they contribute to what is known as the enhanced permeability and retention (EPR) effect.[6–8] Accordingly, there is a great need for new therapeutic strategies capable of delivering chemical agents and other therapeutic materials specifically to tumor locations.

Nanocarriers provide a platform to integrate therapy and diagnostics, which is an emerging direction in medical practice. Nanocarriers as a drug delivery provide high therapeutic performance when targeting specific host sites for the treatment of AIDS, hepatitis, tuberculosis, melanoma, and representative inflammatory diseases.[9–11] Stimuli responsiveness such a pH, redox sensitive nanocarriers can be developed for efficient targeted drug delivery.[12–14] Li et al. demonstrated imporved pharmacokinetics profile *in-vivo* for breast cancer cells with the use of liposomal daunorubicin plus tamoxifen.[15] Hua et al. investigated the possibility of using cross linked redox sensitivie Shell and Core Crosslinked Hyaluronic Acid Nanocarriers for Tumor-Targeted Drug Delivery purposes.[16] In parallel with therapy, polymeric multifunctional nanomaterials can be exploited to exhibit distinctive magnetic, electrical, and optical properties for concomitant imaging.[17–21] Nanostructures, both inorganic and organic materials, have unique chemical, physical, and biological functions, and have been extensively studied as biomaterials or bio-functional materials.[22–26]

Nanofibrous scaffolds are artificial extracellular matrices, which provide natural environment for tissue formation.[27] In comparison to other forms of scaffolds, the nanofibrous scaffolds promote cell adhesion, proliferation, and differentiation more efficiently due to having high surface to volume ratio, three dimensional porous architecture, opportunities to tune their properties by varying composition and manufacturing parameters. These make nanofibers suitable for various fields of biomedical engineering such as cell proliferation, drug delivery, wound dressing cosmetic mask, nano-sensor enzyme immobilization, tissue engineering scaffolds and other biomedical applications.[28, 29] Drugs ranging from antibiotic and anti-cancer agents to proteins, aptamer, DNA[30] and RNA[31] have been incorporated into nanofibers.

Electrospinning has gained widespread interest as a potential polymer processing technique to produce ultra-fine polymer fibers for drug delivery applications.[32–34] It has been proven a relatively simple and versatile method for producing polymeric fibers with diameters ranging from tens of nanometers to microns.[35–37] Manufacturing nanofibers using electrospinning is highly adaptable for biomedical application since all of the properties of nano-fibers can be effectively controlled by a number of processing parameters, such as applied voltage, polymer flow rate, capillary-collector distance, as well as the surface tension and viscoelasticity of solution.[38–41]

Conventional electrospinning technique incorporates drug by hybridization with polymer and leads to initial burst release, which is not desirable in most cases. Electrospinning using special coaxial spinneret can overcome this limitation by encapsulating the drug within the nanofiber polymer matrix.[42, 43] The coaxial electrospinning technique[44–47] is found to be

more useful in loading of various drug, and bioactive agents in polymers, which are forced through a coaxial capillary channel for electrospinning in presence of applied potential. Investigations have indicated that the coaxial technique of drug delivery systems is particularly useful to protect the drugs, which are easily denatured or decomposed during electrospinning of nanofibrous scaffolds. Moreover a core-shell structure minimizes desorption of drugs from the nanofiber surface and releases the drug via diffusion through the porous architecture as well as biodegradation of matrix. A wide range of polymers can be used in electrospinning. Polycaprolactone (PCL) is an FDA approved polymer for biomedical applications, which can be electrospun to effectively encapsulate drug. Good biodegradation properties of PCL in biological media allow delivering drug over prolonged period at a controlled rate. We are here investigating the properties of this polymer as nanofibers and its applicability as a drug delivery device for anticancer therapy.

EXPERIMENTAL METHODS

Polycaprolactone (PCL) of average molecular weight 80,000 g/mol, Poly Vinyl Alcohol (PVA) of average molecular weight 89–98,000 g/mol were purchased from Sigma Aldrich. Anticancer drug 5-Fluorouracil (FU) of 98% purity was purchased from AK Scientific. Another anticancer drug Paclitaxel was of 98% purity from Chem-express. All other chemicals were of reagent grade and purchased from Sigma-Aldrich unless otherwise specified. NF-500 Electrospinning Unit (MECC, Japan) was utilized for electrospinning process. Ultra coaxial spinneret (Fig. 1), a special concentric nozzle was used for developing coaxial stream core and sheath. 27G needle acted as core nozzle, which was placed concentrically into shell nozzle (0.8 mm). Solutions were pumped to the spinneret using two separate precision syringe pumps and 10 ml NORM-JECT® latex free syringes. Separately attached dehumidifier was attached to control system humidity.

Six sets of FU loaded PCL NanoFibers (NFs) in three different category were fabricated using different solvent system and electrospinning parameter. Dimethylformamide (DMF), Acetic Acid (AA), Formic acid (FA), Chloroform/Trichloromethane (TCM), Trifluoroethanol (TFE) were used as solvent individually and in combinations for core and shell. Solvent systems and electrospinning parameters for all sets of NFs are summarized in Table I. For NF set A (category 1), 140 mg/ml of PCL was dissolved in DMF at 110 °C on a magnetic stirrer. For all other NFs (category 2 and 3), shell solution of 140 mg/ml PCL in a mixture of solvents of 47.5% FA, 47.5% AA, 5% TCM or TFE was used. In case of core solution for NFs set of B and C (category 2), 50 mg/ml of PVA was added in addition to 50 mg/ml FU. Neat PCL was manufactured as a control sample using the sheath solution used to synthesize NFs set A.

Paclitaxel was also encapsulated within PCL nanofibers (Sample G) using coaxial electrospinning. 140 mg/ml of PCL was dissolved in a mixture of solvents of acetic acid, formic acid and chloroform at 47.5:47.5:5 ratios. Paclitaxel was dissolved into formic acid at 5 mg/ml concentration. Solution was electrospun at 19.5 kv and 135 mm tip to collector distance. PCL and Paclitaxel solution was pumped at 0.6 ml/hr and 0.1 ml/hr flow rate respectively.

All NFs were collected on wax paper using flat plate collector at traverse speed of 10 mm/s of spinneret and 150 mm traverse distance to get long and thin nanofiber membrane. Nanofibers were taken out of the wax paper and kept into 50 ml deionized water at 37 °C for two hours to let the nanofibers release any drug attached to its surface. It was then dried in vacuum chamber at 25 °C for 24 hours.

In Vitro Drug Release Test

Six random samples of size approximately 20 × 20 mm were taken from each set of NFs. Weight of the samples of corresponding NF set were noted down. Samples were put into 14 ml of 0.01M Phosphate Buffer Saline (PBS) in centrifuge tubes and preserved in a shaking incubator at 37 °C to allow the NFs to release drug in PBS. The PBS media did not contain any serum. 50 μL of PBS solution were collected from each centrifuge tubes to UV transparent 96 well plate at 24 hours interval to measure the amount of released drug from nanofibers within that time. Vortex mixer was used to make the solution homogenized before taking samples. Samples' absorbance was measured using UV-Vis spectrometer at 265 nm. Absorbance of FU is proportional to its concentration in PBS solution. Concentration of FU was calibrated using 38 solutions of FU at different known concentration. To determine total encapsulated drug within the fiber membrane 15 mg of NFs from each set of NFs were dissolved into 14 ml dichloromethane and their absorbance were measured at 265 nm. Background absorbance of dichloromethane was deducted to get absorbance of 5-FU which were compared with standard FU solution. Drug encapsulation efficiency was determined by comparing the encapsulated drug with the feed rate of drug in fiber manufacturing process.

In Vitro Cytotoxicity Test

Human prostatic cancer cells PC3 were used to test the biocompatibility and cytotoxicity of FU loaded PCL NFs. Human prostatic cancer cells derived from metastatic site (bone) was purchased from ATCC, USA. 57 ml of fetal bovine serum (USA origin purchased from Sigma Aldrich), 7 ml of Penicillin-Streptomycin (purchased from life technologies) and 6 ml of HEPES (purchased from life technologies) was added to 500 ml RPMI-1640 medium (Purchased from fisher scientific). This media is called R+ media. 96 well plate were used to grow PC3 cells. 100 μL of PC3 cells at 8×10^4 cells/ml were added on each wells of 96 well plate for all tests. PC3 cells were incubated at 37° C in a humidified 5% CO_2 atmosphere for 24 hours before performing any test.

All NF samples were sterilized in UV radiation for 30 min prior to cell viability tests. Cytotoxicity tests were performed for neat PCL NFs, pristine FU, NFs set A and D. Each tests were performed in individual well plates to avoid cross contamination. All naofiber samples were sterilized using UV radiation for one hour before performing cytotoxicity test. Neat PCL NFs of 5 × 5 mm dimension were incorporated directly into PC3 cells to investigate biocompatibility of PCL NFs. Biocompatibility test were carried out using 6 replica of neat PCL NFs and 6 pristine PC3 cells as control sample. Cytotoxicity of pristine FU was performed by 11 aqueous solution of FU of concentration $0.33–5.6\times10^{-6}$ μM at 1/3 dilution in each step. FU solutions were directly incorporated into cell culture media. Test was performed in triplicates of each FU concentration.

10 mg NFs were taken from NFs set A and D as sample to perform their cytotoxicity. Both NF samples were immersed into 14 ml R+ media and incubated at 37 °C for an hour. This R + media was later diluted by fresh R+ media at different concentration from $0.33–5.6\times10^{-6}$ μM of FU. These FU loaded media was used for the cell culture of PC3 cells. Ninety six well plates were incubated at 37 ° C in a humidified, 5% CO_2 atmosphere for 48 hours to give sufficient time for the fluorouracil to inhibit essential biosynthetic process of the PC3 cells and thus cause them to suicide or cell apoptosis. Antimetabolite drug takes 2–5 days to cause a cell to die. After 48 hours, well plates were taken out from incubator and 20 μL of MTS-based Cell Titer solution was added in each well. MTS based cell titration is a convenient colorimetric method to determine the number of viable cell in cytotoxicity assay. Well plates were kept again in CO_2 incubator for 3 hours and then their absorbance were measured at 490 nm using UV-Vis spectrometer. Absorbance of cells with different concentration of drug was compared with the absorbance of PC3 cells with no drug to determine the cell viability. Percentage of cell viability was plotted against drug amount, which indicates the killing curve of neat FU, NFs set A and D.

Paclitaxel loaded nanofibers were tested in human breast cancer cells for 72 hours. The drug paclitaxel was delivered in thin film-like forms as Paclitaxel-PCL. They were then cut into small 3 mm × 3 mm square pieces that weighed 0.0576 mg containing 0.002592 mg of Paclitaxel for Paclitaxel-PCL. These small pieces were then stored in 100 mm petri dishes and disinfected inside the biosafety laminar flow hood with ultra violet (UV) light for 18 hours.

MDA-MB-231 breast cancer cells (4×10^4 cells) per well were seeded in 24 wells plate. The cells were maintained in 500 μl DMEM-high glucose media with 10% FBS and incubated at 37 °C for 24 hours in normoxia chamber (21% O_2, 5% CO_2) to allow the cells to attach and get acclimatized to the growth conditions. After 24 hours, the media was aspirated gently and the cells were washed with 1×PBS. 500 μl DMEM-HG fresh media was added to each well gently along the walls. The pieces of NFs containing paclitaxel were added in the increments of one each starting from one piece per well to four pieces per well. Each treatment was performed in duplicates. The cells with the treatments were incubated for 24 hrs, 48 hrs and 72 hrs following which images were obtained at each time point using an inverted microscope. Cells were cultured with only cancer cells, cells with neat PCL and Paclitaxel loaded PCL nanofibers.

Proliferation Assay

The drug Paclitaxel and 5-FU was delivered in thin film-like forms as Paclitaxel-PCL and Paclitaxel-5 FU-PCL and 5 FU-PCL. They were then cut into small 3 mm × 3 mm square pieces that weighed 0.00065 g containing 0.00004 g of Paclitaxel for Paclitaxel-PCL and weighed 0.00067 g containing 0.0000388 g of 5-FU for 5 FU-PCL and weighed .00062 g containing 0.000031 Paclitaxel and 0.0000124 5-FU. These small pieces were then stored in 100 mm petri dishes and sterilized inside the biosafety laminar flow hood with ultra violet (UV) light for 18 hours.

The WST assay was used as a cytotoxicity assay for the Human Triple Negative Breast Cancer (TNBC) cell line, MDA-MB-231 cell line using Paclitaxel, 5-FU and combination of

Paclitaxel-5FU. 10,000 MDA MB-231 cells were seeded into 96-well plates (costar 3596-Corning Incorporated) in 100 μL of high glucose concentration Dulbecco's Modified Eagle Medium (DMEM) supplemented with 10% fetal bovine serum, 4.0 Mm L-Glutamine and 4500 mg/L Glucose as provided by the manufacturer (Thermo Scientific). There were total five experimental conditions—(i) control, (ii) PCL fiber only, (iii) PCL and Paclitaxel, (iv) PCL and 5-FU, (v) combination of PCL, Paclitaxel and 5-FU. A chipped piece of drug (as mentioned in the preparation of paclitaxel section above) from each formulation was added into the corresponding well. Each treatment was performed in triplicates for achieving statistical significance. The cells with the treatments were incubated at 37 °C in a normoxia (21% O_2) chamber for 24 hours. After 24 hours the chipped piece of drug was removed from each well. Then 10 μL of WST-1 reagent (ROCHE) was added to each well and incubated at 37 °C in a normoxia (21% O_2) chamber for 4 hours in dark. The remaining viable cells with WST dye uptake were determined by measuring the optical density at 490 nm in Perkin Elmer Wallac *1420 Victor* Multilabel Counter.

Trypan Blue Exclusion Test of Cell Viability

Trypan Blue dye exclusion test was used to discriminate between viable and non-viable cells. 100,000 Human Triple Negative Breast Cancer (TNBC) cell line, MDA-MB-231 were seeded into 24-well plate (costar 3527-Corning Incorporated) in the same media with the same conditions. After 24 hours, all cells (both floating and attached cells) were collected and the viability was determined under bright field microscope by adding trypan blue dye. Dye positive cells are considered dead cells.

RESULTS AND DISCUSSIONS

Morphology analysis of NFs was performed using Scanning Electron Microscopy (SEM) and Energy Dispersive X-ray Spectroscopy (EDS). Samples of 5 × 5 mm dimension were taken for this purpose and gold sputtered for 1 min to form a thin layer of gold on the NFs surface. SEM image of neat PCL NFs (Fig. 2(A)) exhibited thin fibrous network of narrow size distribution ranging from 80–120 nm. Neat PCL NFs exhibited no presence of beads or bundles of fibers. While FU was introduced to the core of NFs during the electrospinning process using same solvent system (NFs set A), it started forming large beads of 0.3–1.2 μm (Fig. 2(B)) within the fiber network. Although NFs set A demonstrated similar fibrous network (Fig. 2(C)) between beads with slight broad diameter range from 50–160 nm at average diameter of 120 nm and standard deviation of 29.6 nm.

SEM images of NFs set A did not demonstrate any FU particles or crystal on surface of NFs which was further verified by EDS. SEM images of NFs set B is shown in Figure 2(D). NFs were randomly distributed and showed non-uniform surface features with lots of FU particles attached to the surface. SEM image didn't exhibit large beads as found in NFs set A, but it exhibited some FU drug particles attached to the surface of NFs which is red marked in the image. Diameter of NFs were distributed between 120–350 nm at average diameter of 238 nm and standard deviation of 92 nm. SEM image of NFs set C is shown in Figures 2(E) and (F). NFs C demonstrated similar morphology as NFs set B. Diameter of fibers were broadly distributed between 60–310 nm at average diameter of 170 nm and

standard deviation of 60 nm. NFs set C exhibited few bundles of fibers within nanofiber matrices and FU drug particles on the surface which is red marked on the image. EDS plot of NFs set B and C is shown in Figures 3(A) and (B) respectively. EDS characterization was performed to determine the presence of Fluorine (F) in the spectra. EDS plot verifies the presence of Fluorine i.e., fluorouracil drug on the surface of NFs set B and C. NFs set C exhibited 4.9 weight percentage of Fluorine on the surface of nanofiber membrane which 1.75 times more Fluorouracil than that of NFs set B.

SEM images of NFs set D, E and F is shown in Figure 4. All of these NFs share similar morphology. None of them showed any formation of large beads, bundles of fibers or presence of FU drug within nanofiber matrices. NFs set F exhibited more uniform surface while NFs set A exhibited less uniform fibers (Figs. 4(E, F)). Diameter of fibers of NFs set D ranged from 110–270 nm at average diameter of 170 nm and standard deviation of 41 nm (Figs. 4(A, B)). NFs set E exhibited diameter ranging from 120–350 nm at average diameter of 200 nm and standard deviation of 57.5 nm (Figs. 4(C, D)). NFs set F showed diameter ranging from 140–400 nm at average diameter of 220 nm and standard deviation of 53.8 nm (Figs. 4(E, F)). SEM images of this three sets of NFs demonstrated fiber diameter increases from D to F. EDS characterization was performed to determine presence of any Fluorine i.e., FU drug particles. EDS plot exhibited no presence of drug particles on the surface of NFs.

SEM image of Paclitaxel loaded PCL nanofibers were shown in Figures 5(A) and (B). SEM images of Paclitaxel loaded PCL nanofiber exhibited thin nanofibers with rough surface properties. Diameter of nanofibers were randomly distributed from 22–90 nm at average diameter of 46.8 nm and standard deviation of 17.2 nm. Paclitaxel loaded PCL nanofibers exhibited narrowest average diameter among all manufactured nanofibers. Diameter distribution plot of paclitaxel loaded PCL NFs is shown on Figure 5(C).

In order to investigate core-sheath structure of drug loaded nanofibers Transmission Electron Microscopy (TEM) was performed. Nanofibers manufactured with Paclitaxel and 5-FU as core and PCL as the sheath outer structure doesn’t contain any metallic compound. Due to absence of metallic compound in the core and sheath TEM/SEM image doesn’t create any contrast difference between core and sheath structure. To overcome this limitations NaCl was added to polymer sheath and another cancer drug Cisplatin (contains platinum) was added along with FU in the core solution. All other solution processing and electrospinning parameters were kept as same as NFs set F. Nanofibers were electrospun directly on TEM grid and dried in vacuum chamber for 24 hours. TEM image as shown in Figure 6 exhibited drug core of app 80–90 nm and polymer sheath of 30–40 nm thickness.

Morphology of coaxial nanofibers largely depends on the solution properties, mutual interaction of polymer as well as drugs. Conductivity difference, viscosity difference, surface tension and volatility of solvents are some of the important physical properties which affects uniformity of core-sheath nanofibers. Viscosity and surface tension difference between solutions dictates Rayleigh instability or jet breakup which primarily determines the presence (or absence) of beads. Additionally core solvent needs to be more volatile than that of shell for stable coaxial NFs formation. Low vapor pressure of core solution tends to retain unevaporated solvent which is responsible for swelling of fibers to form large beads. Core

solution of category 1 NFs was FU in DMF had high conductivity and very low viscosity than that of sheath which resulted in high pulling force inside of a viscous sheath PCL solution. Also DMF has very low volatility in comparison to FA. As a result core solution tends to coagulate which significantly influenced formation of beads within the network of NFs. Neat PCL NFs didn't exhibit any beads since there wasn't any core solution to cause viscous drag and jet breakup. Other categories didn't demonstrate any significant bead formation because solvent for core was more volatile and less conductive to electricity.

Category 2 NFs exhibited accumulation of drug particles outside of fibrous structure. Both of these experienced higher electric potential (1.76 KV/cm and 2.109 KV/cm) in comparison to other NFs set when voltage is considered as a function of tip to collector distance. Such high electric potential causes free charges or ion to migrate very rapidly from core fluids and core-sheath interface to the free surface of the shell. Such rapid migration of charges results in penetration of shell layer since FU solution is polar in nature and can carry ion. When applied voltage is low, charge accumulation occurs primarily on the shell solution and the compound solution droplet at the tip of the spinneret can be expected to remain stable. The electrospinning process can then proceed via charge repulsion at the surface of the shell solution. Entrainment of the core solution can subsequently occur through viscous dragging and contact friction at the interface (of both solutions). Core solution for NFs set B and C also contains PVA in addition to drug which increases its surface tension. FU and PVA are not mutually miscible. PVA possesses higher electrospinability while drug solution alone tends to spray. The combined effect of high electrical stresses, surface tension and presence of PVA resulted in poor drug encapsulation for NFs set B and C. Figure 7 demonstrates the correlation between drug encapsulation efficiency and effective applied voltage. From the correlation it can be seen that drug encapsulation efficiency increase with the decrease of applied voltage. Although NFs set A exhibited comparatively lower encapsulation efficiency even lower voltage because of different solvent system. SEM images (Figs. 3 and 4) also demonstrated that below 65% encapsulation efficiency, drug particles become prevalent outside of nanofiber matrices.

Formic acid, acetic acid and TFE can individually be used as a solvent for PCL which results in different NF morphology due to the variation of conductivity, viscosity of resulting solution and volatility difference. None of these solvents provides good encapsulation with uniform thin fibrous structure when they are used alone. 1:1 ratio FA and AA combination provides better fiber morphology in case of neat PCL NFs synthesis. But when perform coaxial electrospinning with drug solution (FU in FA), this combination results in thick and very uneven NFs because both solution have similar conductivity. TFE has higher conductivity than AA or FA. So, incorporation of TFE into the polymer solution increases its conductivity which resists Raleigh instability and Taylor cone breakup. Conversely incorporation of TFE also increases volatility of solvent system in comparison to core solution because of its higher vapor pressure which increase NFs diameter. So, amount of TFE was optimized to balance between conductivity and volatility of polymer solution. In our experiment, 5% (v/v) TFE resulted in better NF morphology while all other parameters were kept constant. DMF, Tetrahydrofuran, Dichloromethane, Trichloromethane solvents and their combination were also used for dissolving PCL but none of them resulted thin and uniform fibrous structure as in Figures 2 and 3.

Flow rate ratio of shell and core solution also has influence on the stability of compound Taylor cone, diameter of coaxial NFs. Increasing core flow rate increase drug encapsulation in cost reduced encapsulation efficiency and extended nanofibers diameter. Dependency of coaxial NFs diameter on sheath and core flow ration is presented in Figure 8. Electrospinning parameter were not of same, so it is difficult to obtain any rigid dependency. However, polynomial trendline demonstrates that flow ratio become more dominant on NFs morphology when its value is high (>5). On the other when flow ratio is low (such as 1–3) then electrospinning parameters, solution properties, mutual interaction etc. becomes more dominant and flow insignificant influence on morphology.

In-vitro drug release of all sets of NFs for 25 days in PBS media is shown in Figure 9. Category 1 and 3 NFs exhibited steady and consistent release pattern throughout the entire testing period. NFs set A, category 1 showed little bit of high release on the first day while NFs set F, category 3 didn't release significant FU within first day. After first day of drug release NFs set A, F exhibited very similar release pattern though percentage of released drug from NFs set A were approximately 10% higher than NFs set F. On the other hand category 2, NFs set B and C exhibited very high drug release percentage during the initial time period. Both of them released 52–53% of encapsulated within three days of release test while NFs set A, D, E and F released only 13–23% drug. Drug release rate of NFs set B and C were significantly reduced after 3rd day while other sets of NFs showed consistent release pattern. Drug encapsulation efficiency of NFs set A, B, C, D, E and F were determined 70.48%, 62.96%, 52.71%, 73.62%, 72.98%, 77.5% and 76.11% respectively. NFs set B and C exhibited lower encapsulation efficiency since lots of FU particles were attached to the surface of NFs. Drug release from PCL NFs dictated mainly by diffusion of drugs through the pores Disintegration and biodegradation of PCL in PBS media is not that dominant, that's why weight reduction of PCL NFs was insignificant. Drug release characteristics from PCL NFs further depends on the release media itself and its dynamics. Drug release pattern from NFs can also be tuned by using different MW of PCL. Higher MW degrades faster and vice versa. In order to investigate the effect of differential pH level on the drug release characteristics, release tests were performed at different pH level.

In vitro drug release test of FU loaded PCL nanofibers in PBS media at different pH is shown in Figure 10. Four different pH level (7.0, 6.5, 5.8 and 3.0) of PBS media were used. Four sets of FU loaded PCL nanofiber samples were tested at each pH level. The results of the release tests are shown in Figure 10. As demonstrated in the Figure 10, effect of pH was prevalent from the starting of drug release period. It is observed that, % of drug release shows an increasing trend with decreasing pH level of the PBS solution. We believe lower pH level increase the degradation rate of nanofibers which expedites release rate. NFs released least amount of drug in 7.4 pH and drug release rate increase significantly while pH was reduced from 7.4 to 7.00 pH and 6.50 pH. NFs exhibited almost similar release pattern at 6.5 and 5.8 pH. It is also observed that drug release rate increased significantly with slight change of pH from 7.4. But when the pH of PBS is already low (such as 5.8), it requires a significant change of pH to increase a small amount of drug release rate. For example in our experiment on 4th day of drug release test, only 0.4 decrease of pH from 7.4 to 7.0 increased 15.3% drug release while decrease of 2.8 pH from 5.8 to 3.00 increased only 10.2% of drug release rate.

In-vitro biocompatibility test of neat PCL NFs is shown in Figure 11. Cell viability of PC3 cells in neat PCL was evaluated using MTS assay. Cell viability test showed slightly (about 2%) increased growth of PC3 cell in neat PCL NFs in comparison to PC3 cells without any NFs. This further demonstrates that PCL NFs itself not toxic to cells. Nanofibers possess three dimensional architecture which is more favorable to cell growth in comparison to flat bottom cell culture microplate.

In vitro cytotoxicity test of pristine FU, NFs set A and NFs set D is shown in Figure 12. Microscopic images demonstrates PC3 cells at corresponding concentration after 48 hours of exposing NFs to the cell culture media. NFs set A exhibited similar cytotoxic effect to pristine FU while NFs set D demonstrated enhanced efficacy and killing rate. At 5 μM initial drug concentration in the media NFs set D exhibited 38% alive cells while in pristine FU 43% cells were alive and in NFs set A 47.8% cells were alive. With increased concentration of NFs (set D) we have observed the cell viability decreased close to 20%. Drug release from nanofiber matrix relies on diffusion phase from the polymeric matrix along with the biological degradation of the carrier. Diffusion is responsible for initial burst release and in later stage drug release mainly relies on degradation of polymeric shell. In comparison to polylactic acid (PLA), poly glycolic acid (PGA), and other aliphatic polymers, the degradation of PCL in a buffer solution is very slow because of its semi-crystalline nature. Pitt et al. investigated the degradation of implanted, sub-dermal, drug delivery devices produced from PCL (Mn 50,000) over a timescale of 52 months. Weight loss was not recorded until after approximately 2.5 years when the molecular weight (Mn) had fallen to 5000, reflecting the requirement for degraded chain fragments to be below a critical chain length for diffusion from the matrix.

Paclitaxel loaded PCL nanofibers has been tested for cytotoxicity in human breast cancer cells at Georgia Cancer Center, Augusta University. Cancer cells were tested for 72 hours with neat PCL nanofibers and paclitaxel loaded PCL nanofibers in comparison to controlled breast cancer cells. Neat PCL nanofibers showed increased growth while Paclitaxel loaded nanofibers exhibited continuous decrease of number of viable cells. Decrease of viable cells were also dependent on the number of paclitaxel containing NFs. Bright field microscopic images of Breast cancer cells are shown in Figure 13. Continuous decrease of attached cells (cell density) indicated the slow release of paclitaxel from the NF.

Proliferation or cytotoxicity assay showed significantly decreased proliferation in MDA-MB-231 cells treated with PCL+Paclitaxel, PLC+5FU, and PCL+Paclitaxel+5FU compared to that of untreated and cells treated with PCL only (Fig. 14). Similarly, trypan blue dye exclusion test also confirmed the results of WST assay. Number of dead cell varied among the drug treatments. There were 33% dead cells in PCL + Paclitaxel + 5FU treated condition. Both PCL + Paclitaxel and PCL + 5FU treated conditions caused cell death between 40% to 50%.

Acknowledgments

The authors would like to acknowledge support from the National Science Foundation (NSF) for this work through Grant #DMR-1337545 and support from The National Institutes of Health grants # CA160216 and CA172048. We would like to thank Dr. Hao Chen and Dr. Andrew Diamanduros for their assistance in SEM and Cell culture assay.

References

1. Alberts B, Johnson A, Lewis J, Raff M, Roberts K, Walter P. The Molecular Basis of Cancer-Cell Behavior. 2002
2. Hanahan D, Weinberg RA. The hallmarks of cancer. Cell. 2000; 100:57. [PubMed: 10647931]
3. Hanahan D, Weinberg RA. Hallmarks of cancer: The next generation. Cell. 2011; 144:646. [PubMed: 21376230]
4. Baluk P, Hashizume H, McDonald DM. Cellular abnormalities of blood vessels as targets in cancer. Current Opinion in Genetics and Development. 2005; 15:102. [PubMed: 15661540]
5. Nagy, Chang, Shih, Dvorak, Dvorak. Heterogeneity of the tumor vasculature. Seminars in Thrombosis and Hemostasis. 2010; 36:321. [PubMed: 20490982]
6. Greish, K. Cancer Nanotechnology. , editor. Springer; 2010. p. 25-37.
7. Konerding MA, Miodonski AJ, Lametschwandtner A. Microvascular corrosion casting in the study of tumor vascularity: A review. Scanning Microsc. 1994; 9:4.
8. Iyer AK, Khaled G, Fang J, Maeda H. Exploiting the enhanced permeability and retention effect for tumor targeting. Drug Discov Today. 2006; 11:812. [PubMed: 16935749]
9. Ikoba U, Peng H, Li H, Miller C, Yu C, Wang Q. Nanocarriers in therapy of infectious and inflammatory diseases. Nanoscale. 2015; 7:4291. [PubMed: 25680099]
10. Song F, Li X, Wang Q, Liao L, Zhang C. Nanocomposite hydrogels and their applications in drug delivery and tissue engineering. Journal of Biomedical Nanotechnology. 2015; 11:40. [PubMed: 26301299]
11. Nakamae K, Miyata T, Hoffman AS. Swelling behavior of hydrogels containing phosphate groups. Die Makromolekulare Chemie. 1992; 193:983.
12. Zhang X, Zhang H, Yin L, Hu R, Qiu T, Yin Y, Xiong X, Zheng H, Wang Q. A pH-sensitive nanosystem based on carboxymethyl chitosan for tumor-targeted delivery of daunorubicin. Journal of Biomedical Nanotechnology. 2016; 12:1688.
13. Miyata T, Nakamae K, Hoffman AS, Kanzaki Y. Stimuli-sensitivities of hydrogels containing phosphate groups. Macromolecular Chemistry and Physics. 1994; 195:1111.
14. Seki, S., Sakurai, T., Omichi, M., Saeki, A., Sakamaki, D. High-Energy Charged Particles. , editor. Springer; 2015. p. 41-52.
15. Li MH, Yu H, Wang TF, Chang ND, Zhang JQ, Du D, Liu MF, Sun SL, Wang R, Tao HQ, Geng SL, Shen ZY, Wang Q, Peng HS. Tamoxifen embedded in lipid bilayer improves the oncotarget of liposomal daunorubicin *in vivo*. J Mater Chem B. 2014; 2:1619.
16. Zheng H, Yin L, Zhang X, Zhang H, Hu R, Yin Y, Qiu T, Xiong X, Wang Q. Redox sensitive shell and core crosslinked hyaluronic acid nanocarriers for tumor-targeted drug delivery. Journal of Biomedical Nanotechnology. 2016; 12:1641.
17. Peng H, Liu X, Wang G, Li M, Bratlie KM, Cochran E, Wang Q. Polymeric multifunctional nanomaterials for theranostics. J Mater Chem B. 2015; 3:6856.
18. Pietras K, Hanahan D. A multitargeted, metronomic, and maximum-tolerated dose “chemo-switch” regimen is antiangiogenic, producing objective responses and survival benefit in a mouse model of cancer. Journal of Clinical Oncology. 2005; 23:939. [PubMed: 15557593]
19. He W, Cheng L, Zhang L, Liu Z, Cheng Z, Zhu X. Facile fabrication of biocompatible and tunable multifunctional nanomaterials via iron-mediated atom transfer radical polymerization with activators generated by electron transfer. ACS Applied Materials and Interfaces. 2013; 5:9663. [PubMed: 24079826]
20. Suzdalev IP. Multifunctional nanomaterials. Russian Chemical Reviews. 2009; 78:249.
21. WQ, CH, PH, ZH, LPy, LR. Non-genetic engineering of cells for drug delivery and cell-based therapy. Adv Drug Deliv Rev. 2015; 91:125. [PubMed: 25543006]
22. Hanahan, Bergers, Bergsland. Less is more, regularly: Metronomic dosing of cytotoxic drugs can target tumor angiogenesis in mice. Journal of Clinical Investigation. 2000; 105:1045. [PubMed: 10772648]

23. Marshall. Maximum-tolerated dose, optimum biologic dose, or optimum clinical value: Dosing determination of cancer therapies. Journal of Clinical Oncology. 2012; 30:2815. [PubMed: 22753919]
24. Liu M, Li M, Sun S, Li B, Du D, Sun J, Cao F, Li H, Jia F, Wang T, Chang N, Yu H, Wang Q, Peng H. The use of antibody modified liposomes loaded with AMO-1 to deliver oligonucleotides to ischemic myocardium for arrhythmia therapy. Biomaterials. 2014; 35:3697. [PubMed: 24468403]
25. Du D, Chang N, Sun S, Li M, Yu H, Liu M, Liu X, Wang G, Li H, Liu X, Geng S, Wang Q, Peng H. The role of glucose transporters in the distribution of p-aminophenyl-α-d-mannopyranoside modified liposomes within mice brain. J Control Release. 2014; 182:99. [PubMed: 24631863]
26. Cao J, Wang R, Gao N, Li M, Tian X, Yang W, Ruan Y, Zhou C, Wang G, Liu X, Tang S, Yu Y, Liu Y, Sun G, Peng H, Wang Q. A7RC peptide modified paclitaxel liposomes dually target breast cancer. Biomater Sci. 2015; 3:1545. [PubMed: 26291480]
27. Zeng J, Xu X, Chen X, Liang Q, Bian X, Yang L, Jing X. Biodegradable electrospun fibers for drug delivery. Journal of Controlled Release. 2003; 92:227. [PubMed: 14568403]
28. Leung V, Ko F. Biomedical applications of nanofibers. Polym Adv Technol. 2011; 22:350.
29. Xie J, Li X, Xia Y. Putting electrospun nanofibers to work for biomedical research. Macromolecular Rapid Communications. 2008; 29:1775. [PubMed: 20011452]
30. Zhang J, Duan Y, Wei D, Wang L, Wang H, Gu Z, Kong D. Co-electrospun fibrous scaffold–adsorbed DNA for substrate-mediated gene delivery. Journal of Biomedical Materials Research Part A. 2011; 96:212. [PubMed: 21105170]
31. Cao H, Jiang X, Chai C, Chew SY. RNA interference by nanofiber-based siRNA delivery system. J Controlled Release. 2010; 144:203.
32. Zhang Y, Lim CT, Ramakrishna S, Huang Z. Recent development of polymer nanofibers for biomedical and biotechnological applications. J Mater Sci Mater Med. 2005; 16:933. [PubMed: 16167102]
33. Huang Z, Zhang Y, Kotaki M, Ramakrishna S. A review on polymer nanofibers by electrospinning and their applications in nanocomposites. Composites Sci Technol. 2003; 63:2223.
34. Tambralli, Blakeney, Anderson, Kushwaha, Andukuri, Dean, Jun. A hybrid biomimetic scaffold composed of electrospun polycaprolactone nanofibers and self-assembled peptide amphiphile nano-fibers. Biofabrication. 2009; 1
35. Ramakrishna S, Fujihara K, Teo W, Lim T, Ma Z. An introduction to electrospinning and nanofibers. World Scientific. 2005; 90
36. Pillay V, Dott C, Choonara YE, Tyagi C, Tomar L, Kumar P, du Toit LC, Ndesendo VM. A review of the effect of processing variables on the fabrication of electrospun nanofibers for drug delivery applications. Journal of Nanomaterials. 2013 2013.
37. Deitzel JM, Kleinmeyer J, Harris D, Tan NB. The effect of processing variables on the morphology of electrospun nanofibers and textiles. Polymer. 2001; 42:261.
38. Thompson CJ, Chase GG, Yarin AL, Reneker DH. Effects of parameters on nanofiber diameter determined from electrospinning model. Polymer. 2007; 48:6913.
39. Theron SA, Zussman E, Yarin AL. Experimental investigation of the governing parameters in the electrospinning of polymer solutions. Polymer. 2004; 45:2017.
40. Tan SH, Inai R, Kotaki M, Ramakrishna S. Systematic parameter study for ultra-fine fiber fabrication via electrospinning process. Polymer. 2005; 46:6128.
41. Zhang, Huang, Xu, Lim, Ramakrishna. Preparation of core-shell structured PCL-r-gelatin bi-component nanofibers by coaxial electrospinning. Chemistry of Materials. 2004; 16:3406.
42. Absar S, Khan M, Edwards K, Neumann J. Investigation of synthesis and processing of cellulose, cellulose acetate and poly (ethylene oxide) nanofibers incorporating anti-cancer/tumor drug cis-diammineplatinum (II) dichloride using electrospinning techniques. Journal of Polymer Engineering. 2015; 35:867.
43. Absar S, Khan M, Edwards K, Calamas D. Electrospinning of Cisplatin-Loaded Cellulose Nanofibers for Cancer Drug Delivery. 2014 V009T12A085.
44. Jiang H, Hu Y, Li Y, Zhao P, Zhu K, Chen W. A facile technique to prepare biodegradable coaxial electrospun nanofibers for controlled release of bioactive agents. J Controlled Release. 2005; 108:237.

45. Jiang H, Wang L, Zhu K. Coaxial electrospinning for encapsulation and controlled release of fragile water-soluble bioactive agents. J Control Release. 2014; 193:296. [PubMed: 24780265]

46. Song T, Zhang Y, Zhou T, Lim CT, Ramakrishna S, Liu B. Encapsulation of self-assembled FePt magnetic nanoparticles in PCL nanofibers by coaxial electrospinning. Chemical Physics Letters. 2005; 415:317.

47. Zhang Y, Huang Z, Xu X, Lim CT, Ramakrishna S. Preparation of core-shell structured PCL-r-gelatin bi-component nanofibers by coaxial electrospinning. Chemistry of Materials. 2004; 16:3406.

SUMMARY

- Anticancer drug FU was encapsulated within PCL nano-fibers (avg dia 190 nm) and Paclitaxel was encapsulated within ultrafine coaxial nanofibrs (avg dia 46.8 nm).
- Addition of TFE with formic acid and acetic acid as solvent for polymer sheath influenced formation of narrow NFs.
- Incorporation of PVA in core drug solution resulted in nanocrystals outside of sheath surface and poor encapsulation (52.71% efficiency). Absence of polymer in core and lower effective voltage (around 1.4 KV/cm) increased drug encapsulation efficiency (77.5%).
- Increase of sheath to core solution flow ratio resulted in decreased diameter of nanofibers. At 1.5 flow ration average fiber diameter was 220 nm while flow ratio 6 resulted 46.8 nm average fiber diameter.
- *In-vitro* cell viability tests showed enhanced cancer cell growth in NFs compare to flat bottom well plate environment. While FU loaded NFs demonstrated increased efficacy in comparison to pristine FU.
- Encapsulated NFs demonstrated consistent drug release pattern for 25 days in PBS media and increased cytotoxicity in comparison to pristine drug when tested in human prostatic cancer and breast cancer cells.
- Cell viability was determined by WST assay and trypan blue dye exclusion test. In both assays, PCL containing paclitaxel, 5-FU and both Paclitaxel and 5-FU decreased cell viability between 33 to 50%.

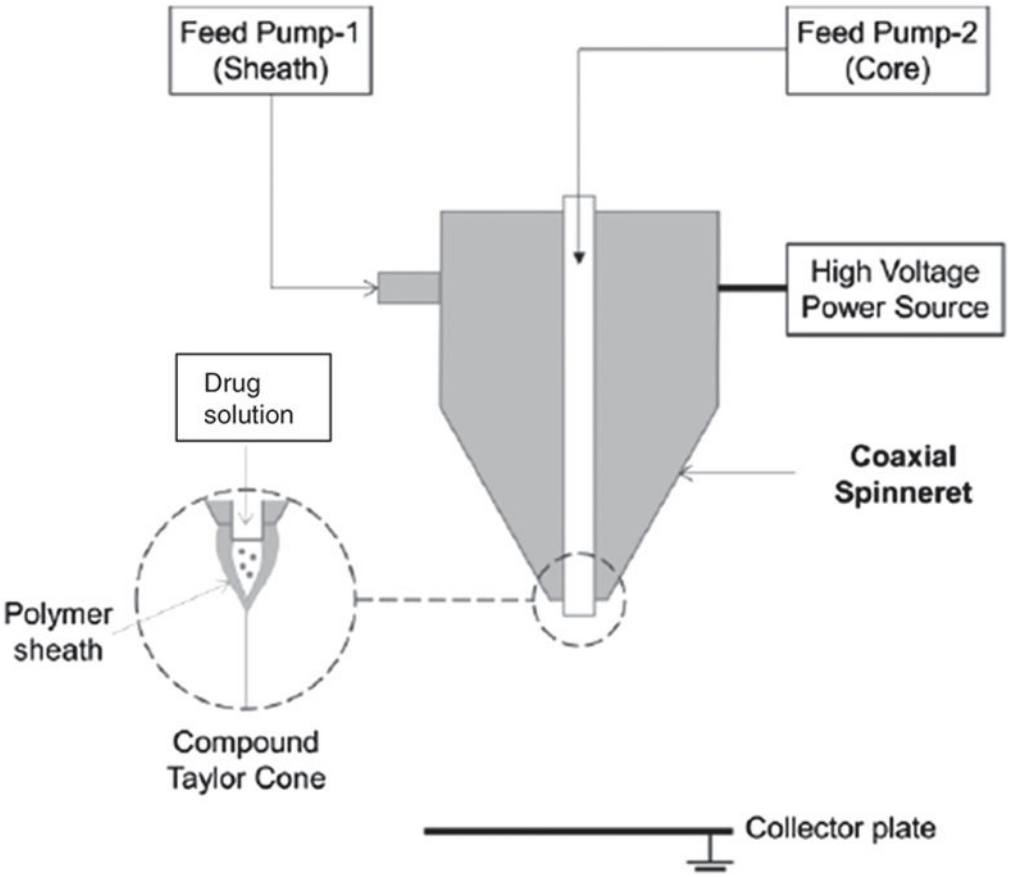

Figure 1.
Schematic representation of ultra coaxial spinneret showing two stream of fluid flow and compound Taylor cone.

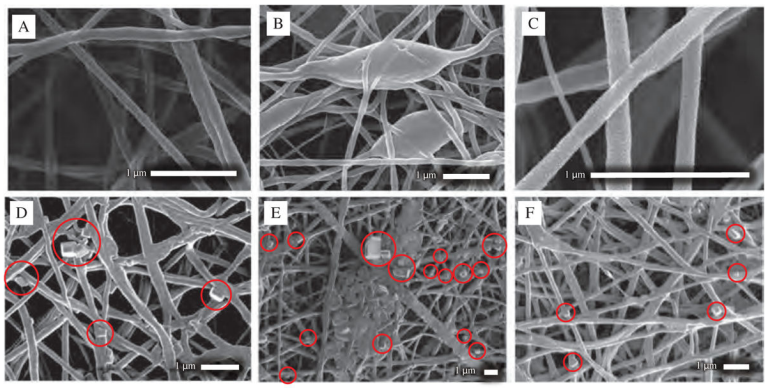

Figure 2.

SEM images of (A) Neat PCL NFs, (B), (C) NFs set A, category 1 at different magnification and location showing beads within fiber network, (D) NFs set B, category 2 at different magnification and location showing presence of FU nanocrystals outside of sheath which is red marked, (E), (F) NFs set C, category 2 at different magnification and location showing presence of FU nanocrystals outside of sheath which is red marked.

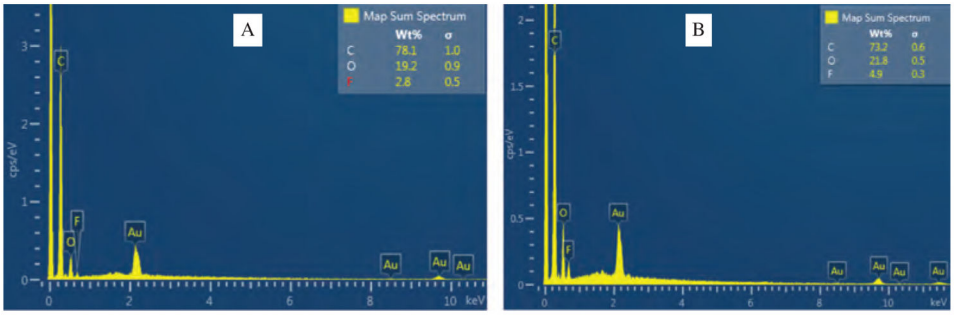

Figure 3.

EDS plot showing weight percentage of Fluorine on the surface of (A) NFs set B, category 2 (B) NFs set C, category 2.

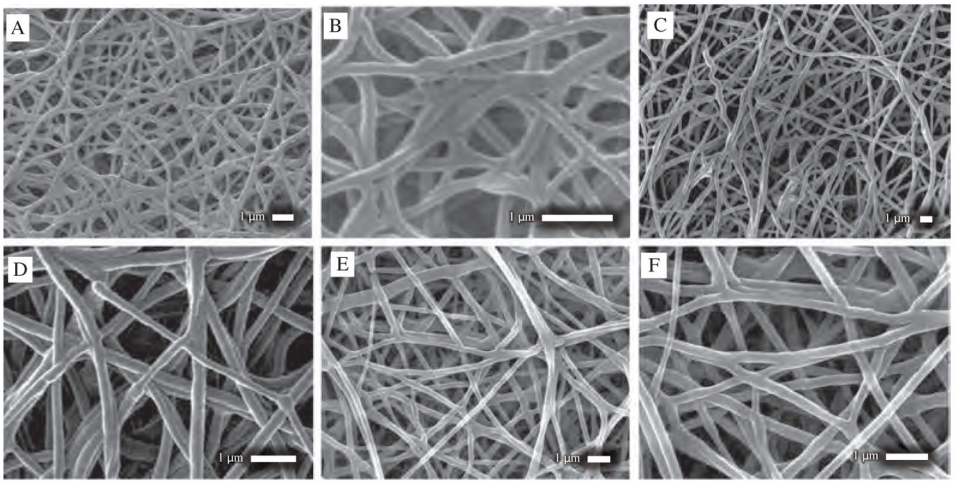

Figure 4.

SEM images of (A), (B) NFs set D, category 3 at different magnification and location (C), (D) NFs set E, category 3 at different magnification and location showing uniform NFs formation without large beads or drug nanocrystals outside of sheath (E), (F) NFs set F, category 3 at different magnification and location showing uniform, thin NFs formation without large beads or drug nanocrystals outside of sheath.

Figure 5.

(A) SEM image of Paclitaxel loaded PCL nanofibers (NFs set G, category 3) showing randomly distributed fibers with no presence of beads or drug particles outside (B) SEM image of Paclitaxel loaded PCL nanofibers showing dimensions of nanofibers (C) Diameter distribution plot of Paclitaxel loaded PCL nanofibers (NFs set G, category 3).

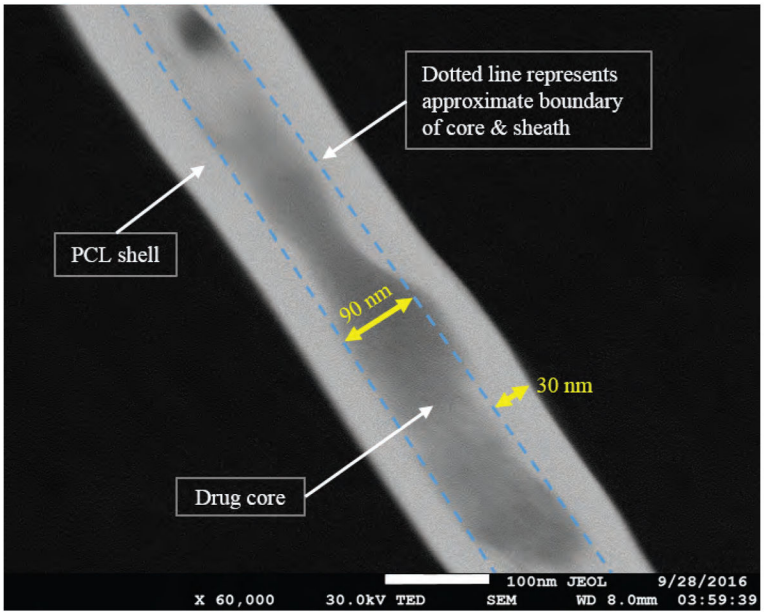

Figure 6.

TEM image of anticancer drug loaded PCL nanofibers showing 5-Fluorouracil, cisplatin encapsulated within PCL sheath. Anticancer drug cisplatin was added in core and NaCl was added to sheath to enhance contrast in TEM image. Dotted line was drawn to demonstrate an approximate boundary between core and sheath.

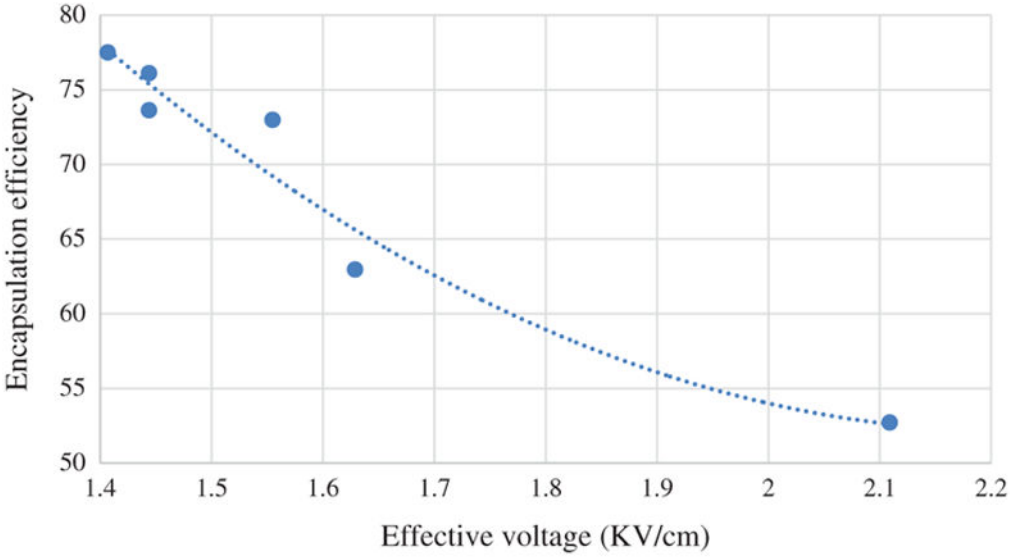

Figure 7.
Graphical representation of correlation between drug encapsulation efficiency and effective applied voltage.

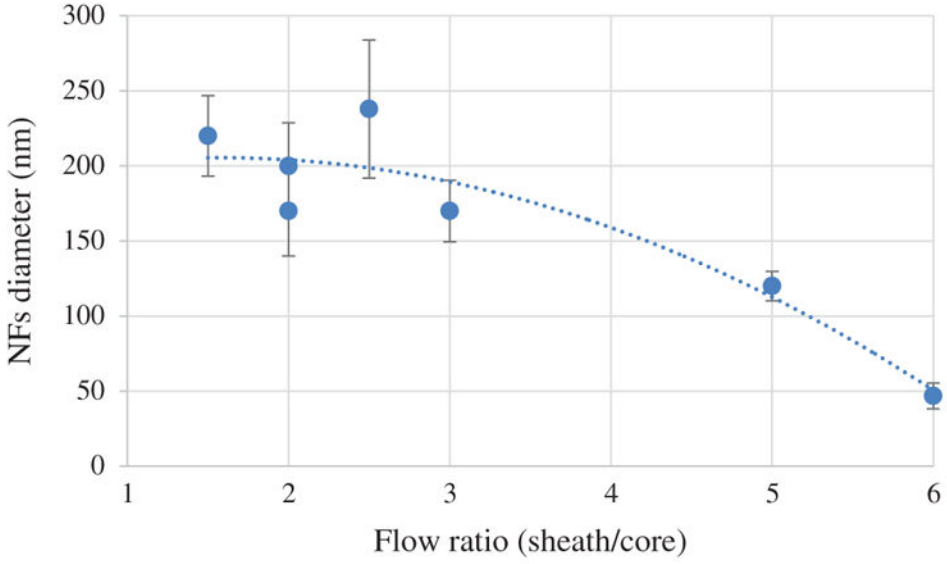

Figure 8.
Graphical representation of Influence of Sheath core fluid flow ratio on NFs diameter.

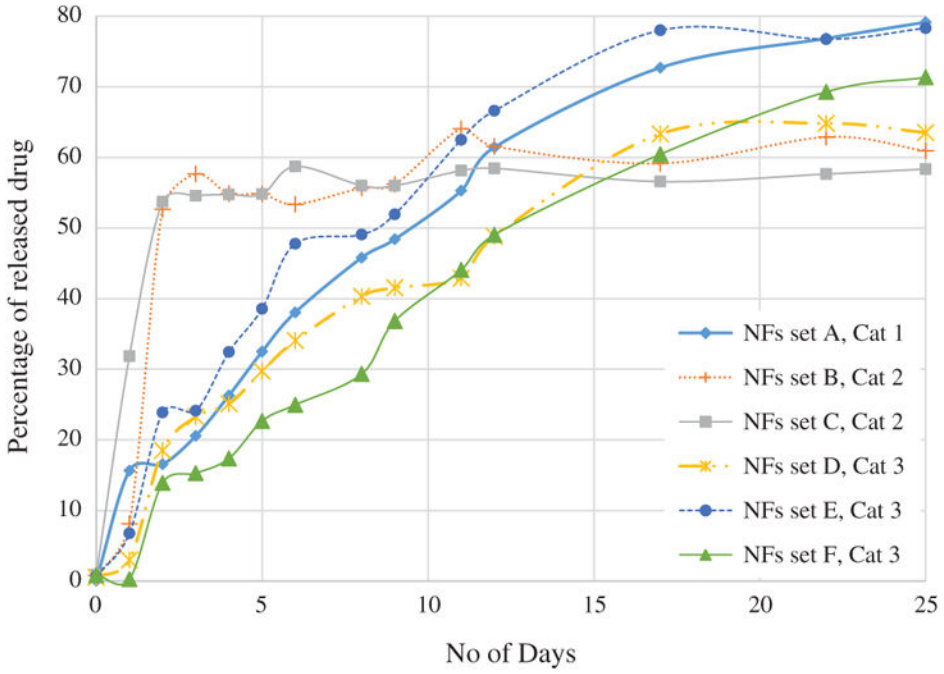

Figure 9.

In-vitro FU drug release test from the drug loaded PCL nanofibers in PBS media for 25 days.

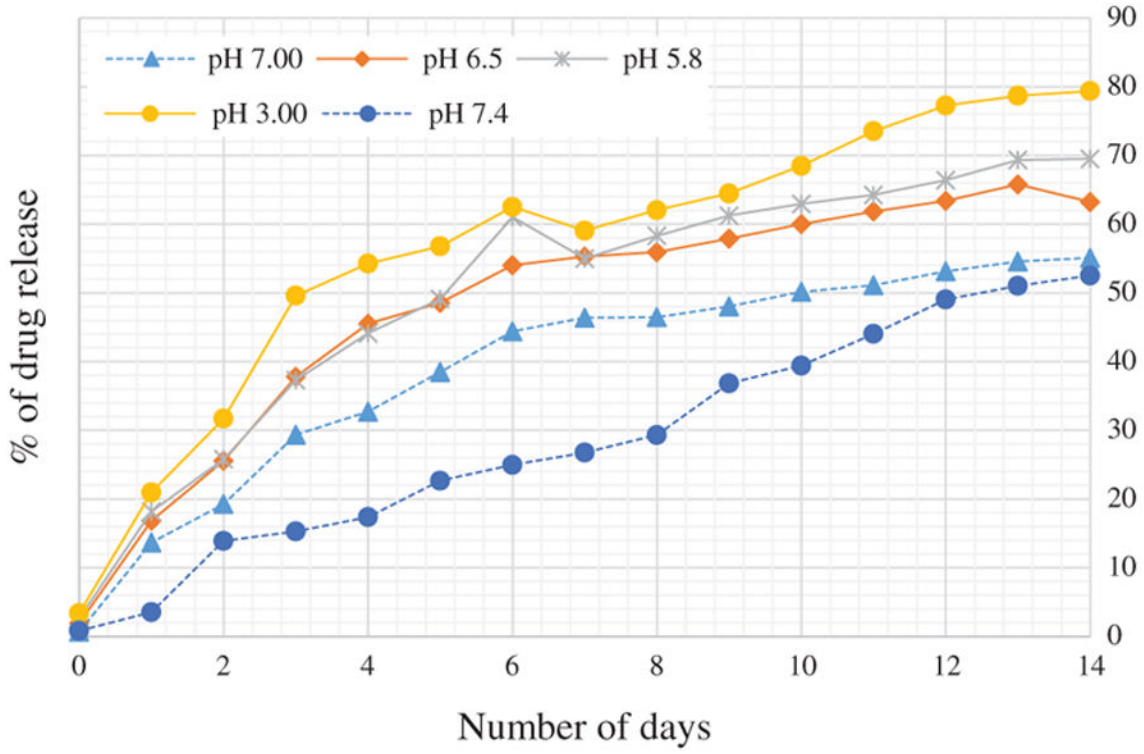

Figure 10.
In-vitro drug release test of FU loaded PCL nano-fibers in PBS media at different pH.

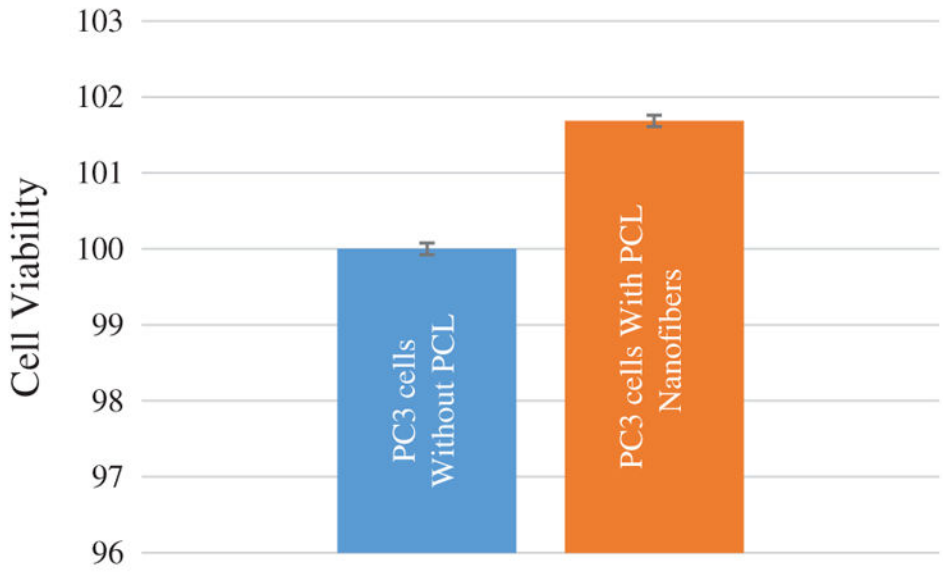

Figure 11.
In-vitro biocompatibility of neat PCL NFs.

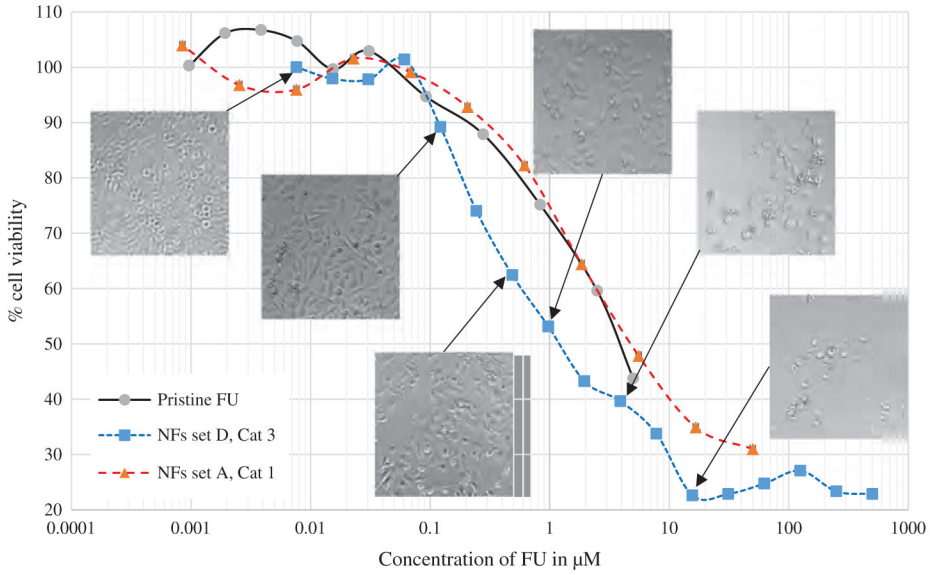

Figure 12.

In vitro cell viability test of PC3 cells in pristine FU, NFs set A and NFs set D. Microscopic images of PC3 cells after 48 hours of cell viability test at corresponding FU concentration.

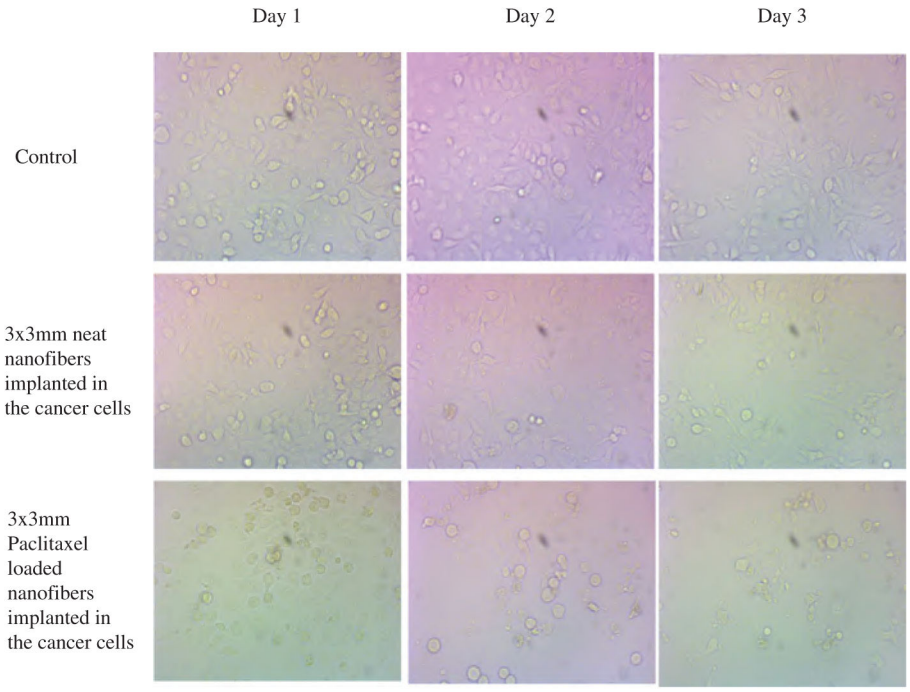

Figure 13.

Microscopic images of breast cancer cells with neat PCL nanofibers (4 piece), paclitaxel loaded nanofibers (4 piece) (NFs set G, category 2).

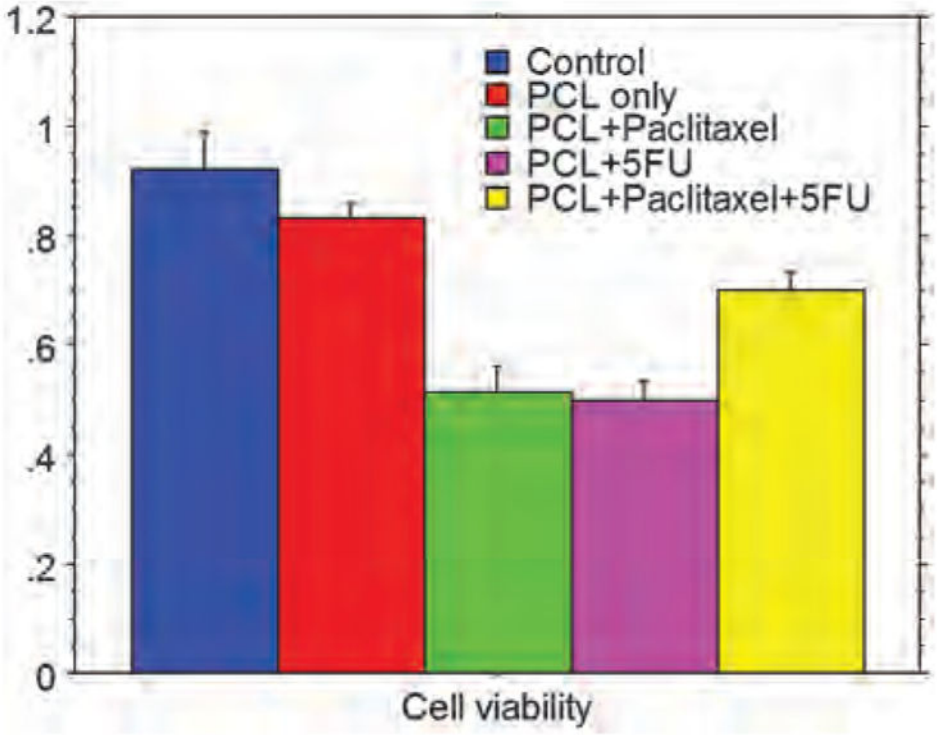

Figure 14.

Cell viability (MDA-MB-231 triple negative breast cancer) determined by WST assay (cell proliferation). There was significantly decreased viability in cells treated with PCL +Paclitaxel, PCL +5FU, and PCL +Paclitaxel+5FU.

Table I

Solvent systems and electrospinning parameter for FU loaded PCL NFs.

		Core solution			Sheath solution				
NFs set	**Category**	**Solvent**	**Solute (mg/ml)**	**Flow rate (ml/hr)**	**Solvent**	**Solute (mg/ml)**	**Flow rate (ml/hr)**	**Applied voltage (KV)**	**Tip to collector distance (mm)**
Neat PCL	1	Not applicable	Not applicable	Not applicable	DMF	140 mg/ml PCL	1	21	185
A	1	DMF *	50 mg/ml FU ‡	0.2	DMF	140 mg/ml PCL	1	21	185
B	2	FA †	50 mg/ml FU, 50 mg/ml PVA §	0.4	47.5% FA, 47.5% AA ∥, 5% TCM ¶	140 mg/ml PCL	1	22	135
C	2	FA	50 mg/ml FU, 50 mg/ml PVA	0.5	47.5% FA, 47.5% AA, 5% TCM	140 mg/ml PCL	1	23.2	110
D	3	FA	50 mg/ml FU	0.2	47.5% FA, 47.5% AA, 5% TCM	140 mg/ml PCL	0.6	19.5	135
E	3	FA	50 mg/ml FU	0.2	47.5% FA, 47.5% AA, 5% TCM	140 mg/ml PCL	0.4	21	135
F	3	FA	50 mg/ml FU	0.2	47.5% FA, 47.5% AA, 5% TCM	140 mg/ml PCL	0.3	19	135
G	3	FA	5 mg/ml Paclitaxel	0.1	47.5% FA, 47.5% AA, 5% TFE #	140 mg/ml PCL	0.6	19.5	135

Notes:

*Dimethylformamide;

†Formic Acid;

‡5-Fluorouracil;

§PolyVinyl Alcohol;

∥Acetic acid;

¶Trichloromethane;

#Trifluoroethanol.

Table II

Characteristics of drug loaded nanofibers.

NFs set	NFs category	Core solution characteristics	Voltage (KV/cm)	Morphology	Flow ratio (Shell/core)	Encapsulation efficiency (%)	Avg dia (nm)
A	1	High conductive and low volatility	1.135	Large beads	5	70.48	120
B	2	Low conductive, high volatility, contains PVA *	1.629	Outside drug particles	2.5	62.96	238
C		Low conductive, high volatility, contains PVA	2.109	Outside drug particles	2	52.71	170
D	3	Low conductive, high volatility	1.444	Uniform	3	73.62	170
E		Low conductive, high volatility	1.555	Uniform	2	72.98	200
F		Low conductive, high volatility	1.407	Uniform	1.5	77.5	220
G		Low conductive, high volatility	1.444	Uniform	6	76.11	46.8

Note:

* Polyvinyl alcohol.